Proceedings World Geothermal Congress 2010
Bali, Indonesia, 25-29 April 2010

Heat Transfer in Geothermal System of Mutnovsky Volcano: the Influence of the Form, Discharge of Magma Chamber Degassing and Rocks Permeability

Roman I. Pashkevich and Vitaly V. Taskin

SRGC FEB RAS, Severo-vostochnoe shosse, 30, Petropavlovsk-Kamchatsky, 683002, Russian Federation

teplosnab@rambler.ru, taskin-v@yandex.ru

Keywords: geothermal system, supercritical fluid, magma chamber, numerical simulation, HYDROTHERM

ABSTRACT

A thermohydrodynamic model of the magma-geothermal system of the Mutnovsky volcano was developed. The temperatures and hydrodynamic fields in the fluid conduction zone and volcanic edifice were calculated. Both convective and conductive heat transfer in the rocks were considered. The influences of rock permeability, depth of the magma chamber, and fluid pressure on the process character were investigated. The possible range of chamber depths was calculated.

1. INTRODUCTION

Lately, the numerical simulation of hydrovolcanic, hydrothermal, and magmatogene-geothermal processes has been developed intensively for volcano-geothermal systems. The HYDROTHERM code developed by Hayba and Ingebritsen (1994) is the most commonly used. HYDROTHERM is assigned for the three-dimensional simulation of multiple flows of water and heat in permeable media with temperature and pressure ranges of 0–1200°C and 0.05–1000 MPa, respectively. These ranges of conditions are appropriate for such geothermal systems. HYDROTHERM was used to simulate

- Magma-hydrothermal and volcano-hydrothermal systems of the Cascade Range volcanoes in the USA to clear up how the location of underground waters in volcano edifices influences system regimes (Hurwitz *et al*. 2003);
- Explosions of the Maion volcano edifice in the Philippines, due to the magma intrusion heating (Reid 2004);
- Volcanomagnetic effects observed in volcanoes in Aso, Japan due to hydrothermal activity (Okubo *et al*. 2004);
- Magma-hydrothermal systems of Unzen volcano in Japan (Fujimitsu *et al*. 2005);
- Changing of heat regime of magma-hydrothermal system of Kuju volcano system, Japan, after phreatic eruption of 1995 (Ehara *et al*. 2005).

2. THE OBJECT AND ITS CHARACTERISTICS

The Mutnovsky volcano is a large polygenic active volcanic edifice appeared in the Pliocene-early Pleistocene. Vakin showed (1966) that it is a complex massif with a maximum altitude of 2323 m. In the western part of the massif, there is a depression with eight form in plan and a long axis that extends to the Northeast. It was formed by the merging of two craters, each with a diameter of about 1.5-2.0 km. The southwest crater is occupied by glaciers, and the most northeastern part of the crater contains Bottom and Upper active fumarole fields. The most intensive fumarole activity is in a small crater called the Active Crater (AC).

2.1 Conceptual Model

After the eruption and during the completion phase of the volcano cone and the Active Crater formation, magma completely fills a vent conduit and begins to cool due to heat loss to the environment. Contraction fractures appear in the conduit, increasing its permeability. The fractures are paths for fluid formed in an apical part of chamber during the degassing of constantly convecting magma. Thermal and hydrodynamic interactions of fluid and water of the volcanic rocks is observed during the filtration along the fluid-conductive zone (FCZ). As a result, fumarole volcano activity is formed.

2.2 Thermohydrodinamic Model

Standard equations of mass and energy conservation in permeable mediums were used as given by Hayba and Ingebritsen (1994):

$$\frac{\partial(n\rho_f)}{\partial t} - \nabla\cdot\left[\frac{kk_{rs}\rho_s}{\mu_s}(\nabla p - \rho_s \boldsymbol{g})\right] - \nabla\cdot\left[\frac{kk_{rw}\rho_w}{\mu_w}(\nabla p - \rho_w \boldsymbol{g})\right] - q_m = 0 \quad (1)$$

$$\frac{\partial}{\partial t}\left[n\rho_f h_f + (1-n)\rho_r h_r\right] - \nabla\cdot\left[\frac{kk_{rs}\rho_s h_s}{\mu_s}(\nabla p - \rho_s \boldsymbol{g})\right] - \nabla\cdot\left[\frac{kk_{rw}\rho_w h_w}{\mu_w}(\nabla p - \rho_w \boldsymbol{g})\right] - \nabla\cdot K_m \nabla T - q_h = 0 \quad (2)$$

where n is porosity; ρ_f, ρ_s, and ρ_r are fluid, steam and rock densities, respectively; k is the absolute permeability; k_{rs} and k_{rw} are the relative permeabilities of steam and water, respectively; μ_s,and μ_w are the dynamic viscosities of steam and water, respectively; K_m is thermal conductivity; h_f and h_r are the enthalpies of fluid and rocks, respectively; and q_m and q_h are the mass and heat flowrates of sinks and sources, respectively.

2.3 Schematization of Environmental Conditions. Geometry of Model Region

The geothermal magma system of the Mutnovsky volcano is considered to be a fracture-and-porous vertical zone with a thickness equal to a lateral dimension of the Active crater (150 m). The zone stretches to the north-northeast and passes through the axis of the Active crater. A two-dimensional model was used for calculations. The depth of modeled region varies depending on the depth of the accepted apical part of the magma chamber. The fluid-

conductive zone is a vertical flat passing through the line which connects the center of the Active crater, the Bottom field, and the Upper field.

2.4 Initial and Boundary Conditions

An average geothermal gradient of 30°C/km and hydrostatic distribution of fluid pressure were assigned as the initial conditions of the rocks surrounding the magma chamber. A regional heat flow of 120 mW/m^2 was given at a lower boundary of the simulation domain; constant pressure (atmospheric) and temperature (10°C) were assigned on the upper boundaries outside the Active crater; and atmospheric pressure was specified on the surface of the Active crater. An absence of fluid flow at the side boundaries was assumed. A constant temperature of 900°C was assigned at an inner surface of the constantly convecting chamber.

2.5 Magma Chamber Volume and Form

Using a lower bound of magma chamber degassing and discharge volume of 10 km^3 in accordance with data of Trukhin (2003), a minimum radius of 1.2 km was obtained for magma chamber with a spherical form. The mean radius of the Mutnovsky Upper chamber was determined to be 1.5 km by Utkin *et al.* (2005) after all geological, geophysical, geomorphological, remote, petrological and geothermal data were considered. The two aforementioned estimations are similar. The radius of the chamber with a spherical shape was assigned to be equal to 1.5 km. In calculations, the chamber was assumed to have the shape of a horizontal ellipse. The lengths of the ellipse's semi axes were calculated under the conditions of equal values of the spherical and ellipsoid chambers.The main cross-sectional area of the ellipsoid was given to be equal to that of the sphere (7.1 km^2). The major semiaxis of the ellipse (2.2 km) was found to be twice as large as the minor semi axis (1.1 km).

2.6 Time of Active Fumarole Activity of Volcano and Simulation Time

The active crater formation is connected to explosive sediment of the age 1.2–1.3 Ma (Selyangin 2007). Thus, the simulation time was assigned to be 1.2 Ma. The simulation time in one of the variants was increased to 10 thousand years to study the dynamics of a complete process.

2.7 The Temperature of Chamber Apical Part

As estimated by Utkin *et al.* (2005), the temperature of magma flowing out of the Mutnovsky Upper chamber is 900°C (the melting temperature of host rocks), and the temperature of magma flowing into the chamber is 1200–1250°C. In the calculations shown, the temperature of the apical part of the chamber was assigned to be 900°C.

The temperatures of gases and fumarole rocks of the Active crater are presented in Table 1. During the observation, the temperature of the Active crater fumaroles varied from 492-950°C.

2.8 Fluid Pressure at the Point of Entry of Fluid-Conductive Zone

Fluid pressure in the apical part of the chamber is indeterminate and it can be estimated in the range from hydrostatic to lithostatic conditions. The pressure at the point of entry of the fluid-conductive zone was assigned within this range in accordance with the accepted chamber depth under the surface of the Active crater (7.5-80 MPa).

Table 1: The temperature of gases and fumarole rocks of the Active crater (Vakin *et al.*, Polyak, 1966; Zelensky *et al.*, 2002–2007)

Date of measurements	Maximum rock temperature (determined by incandescence)	Maximum measured temperature of gases
August, 1963	850 – 900°C	750°C
	1000°C	750°C
August, 1964	800 – 950°C	950°C
1999	N/A	524°C
June – August, 2000	N/A	492°C
2001 - 2002	N/A	520°C
2005	N/A	620°C

2.9 Fluid Flowrate and Entalpy

The flowrate of the fumarole gases of the Active crater is 500 kg/s (Vakin 1966). The flowrate of magma fluid at the point of entry of the fluid-conductive zone was also assigned to be 500 kg/s. The fluid enthalpy at the point of entry of the fluid-conductive zone was determined by the phase diagram of water. Within the aforementioned range of fluid pressures, enthalpy varies insignificantly with a mean value of 4500 kJ/kg along the line of the 900°C isotherm.

2.10 Key Parameters Varying in the Calculations

The main parameters determining the dynamics of thermal and hydrodynamic fields are chamber depth and the permeability of rocks in and around the fluid-conductive zone. The permeability of the fluid-conductive zone (K_{FCZ}) and of rocks surrounding the fluid-conductive zone (K_R) varied within 1–100 and 10^{-4}–1 mD, respectively. The hydrogeological conditions in the volcano edifice have been studied imperfectly in the past, so both convective and conductive heat transfer in rocks surrounding fluid-conductive zone were studied. A high permeability of surrounding rocks was assigned for the former type, and a low value was assigned for the latter type. The density, heat capacity and heat conductivity of rocks were assumed to be constant and equal to average values for volcanic and metamorphic rocks (2500 kg/m^3, 1 kJ/kg, and 2 W/m·K, respectively). The porosity was assumed to be 10%. Thirty-three variants of parameters were used.

3. CONVECTIVE HEAT TRANSFER

3.1 General Dynamics of Process

A convection zone of supercritical fluid develops near the chamber surface, as shown in Figure 1.

Within the fluid-conductive zone and its surroundings, fluid rises first at supercritical conditions up to a depth of 2.2 km, which approximately corresponds to a critical water pressure of 22 MPa. From this depth, fluid rises as superheated steam and exits to the surface. It is partially condensed on the periphery of the superheated fluid zone due to heat loss to surrounding rocks. Outside the steam zones, free convection of water develops in the volcano edifice. It is significant that fumaroles in the Bottom and Upper fields discharge mainly wet steam, and that fumaroles in the Active crater discharge superheated steam. Thus, there is a qualitative coordination of the model and real processes.

3.2 The Influence of Initial Fluid Pressure on the Process Nature

Under the same conditions, the higher initial fluid pressure at the point of entry of the fluid-conductive zone, the wider zone of supercritical convection, and the higher the level of transition from supercritical conditions to superheated steam, rate of rocks warm in surrounding of fluid-conductive zone, rate of supercritical fluid and water. At the same time, the fluid pressure in the zone of supercritical convection increases, as shown in Figure 1.

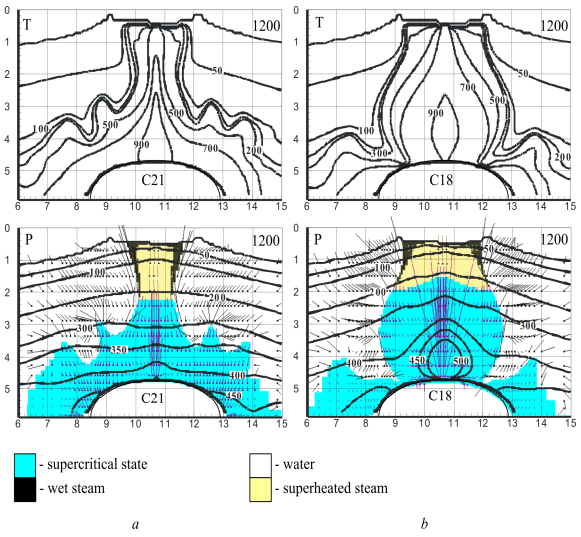

Figure 1: The distribution of temperature (T, ^{o}C), pressure (P, bar), and phase state under convective heat transfer within rocks surrounding the fluid-conductive zone and different fluid pressures in the apical part of the chamber: a – 45 MPa, b – 80 MPa. K_R=1 mD, K_{FCZ}=10 mD.

4. CONDUCTIVE HEAT TRANSFER

4.1 General Dynamics of Process

As a whole, the process is similar to convective heat transfer. However, as a result of a high hydrogasdynamic resistance of edifice rocks, supercritical convection doesn't occur, and the peripheral area of wet steam is absent, as shown in Figure 2. At the same chamber depths and rock permeabilities in the fluid-conductive zone, the mean temperature of the rocks surrounding the fluid-conductive zone is much lower than during convective transfer, as shown in Figures 1 and 2a. It was determined that the fluid temperature in the fluid-conductive zone became steady after 10 thousand years.

4.2 The Influence of Chamber Depth on the Process Nature

If fluid pressure at the point of entry is equal to hydrostatic pressure, the depth of transition of supercritical fluid flow within the fluid-conductive zone doesn't practically depend on chamber depth, and it is almost equal to the depth which corresponds to critical water pressure (2.2 km, 22 MPa), as illustrated in Figure 2. The higher the chamber is located, the higher temperature gradient is in the edifice rocks.

4.3 Dynamics of Fluid Temperatures and Pressure of Fluid-Conductive Zone

The fluid temperature near the surface of the Active crater begins to decrease to a minimum and then increases, as shown in Figure 3. At the same time, the rate of temperature decrease is higher than the rate of the subsequent increase. The period of temperature decline decreases to 300-700 years if the fluid pressure rises at the point of entry of fluid-conductive zone rises. The rates of temperature decline and rise are 0.5 and 0.25^{o}C/year, respectively, and do not depend on pressure. Pressure near the surface of the active crater sharply increases within 30 years, followed by the period of slow decline.

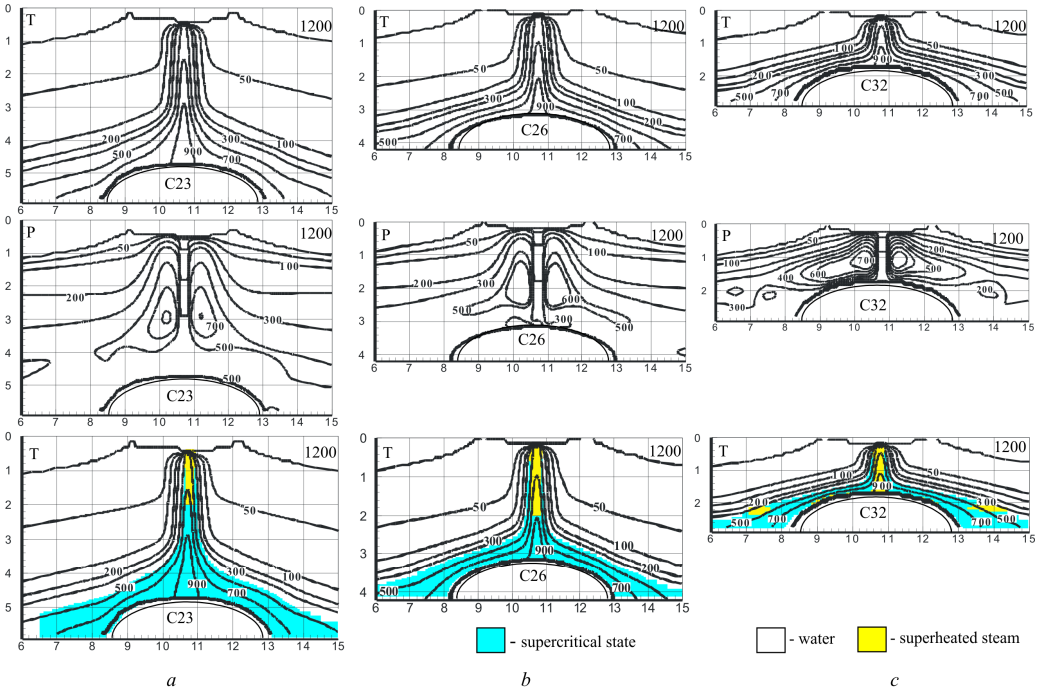

Figure 2: The distribution of the temperature, pressure and phase (from top to bottom) in the models with conductive heat transfer at chamber depths of: *a* – 4.5 km, *b* – 3 km, *c* – 1.5 km. $K_R=10^{-4}$ mD, K_{FCZ}=10 mD. Fluid pressure at the point of entry of the fluid-conductive zone is assigned to be equal to hydrostatic pressure.

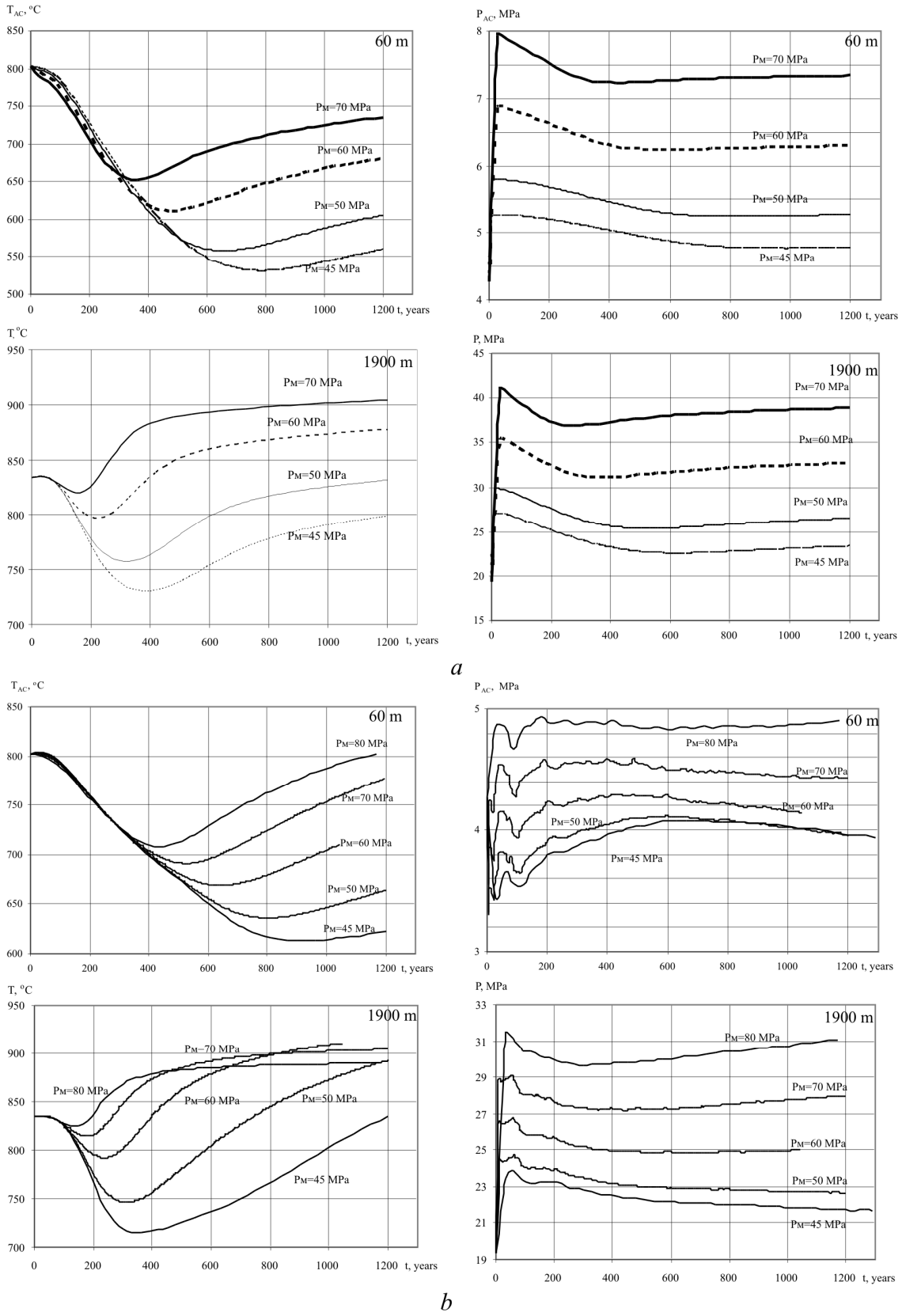

Figure 3: Change of the fluid temperature and pressure over time under different apical chamber pressures (Pм). *a* – conductive heat transfer, $К_R = 10^{-4}$ mD, models C22–C25; *b* – convective heat transfer, $К_R$=1 mD, models C17–C21. $К_{FCZ}$ =10 mD. The depth from the active crater surface is shown in the upper right corner. Chamber depth is 4.5 km.

This period decreases as pressure at the point of entry of the fluid-conductive zone increases, after which the pressure becomes relatively stable. The decompression rate decreases from 2 to 0.7 κPa/year if pressure rises from 45 to 70 MPa at the point of entry of the fluid-conductive zone.

5. TEMPERATURE AND PRESSURE NEAR THE SURFACE OF ACTIVE CRATER

A number of numerical experiments were performed with 27 models to determine the possible chamber depth according

to the actual temperature of gases in the active crater. The results of these experiments are illustrated in Figure 4. If chamber depth is fixed, the fluid temperature near the Active crater increases with fluid pressure. If the pressure at the point of entry of the fluid-conductive zone is fixed, the fluid temperature near the active crater also rises.

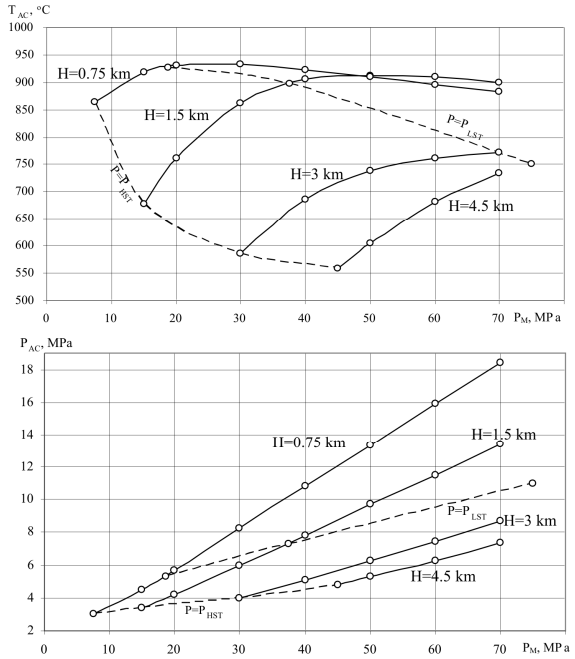

Figure 4: The dependence of temperature (T_{AC}) and pressure (P_{AC}) (the depth is 60 m from Active crater surface) on pressure at the point of entry of the fluid-conductive zone at different chamber depths (H). The period of time is 1.2 thousand years. Heat transfer is conductive. Dashed lines indicate gases with pressures equal to hydrostatic (P_{HST}) and lithostatic (P_{LST}) pressure at the chamber depth. Data was obtained using models C22–C30, C32–C34, C39–C50.

The true value of fluid pressure at the point of entry of the fluid-conductive zone is not known, and the mean value of the lithostatic and hydrostatic pressures at the depth of the apical part of the chamber is a reasonable estimate. In that case, if weight-average temperature value of the active crater gases over an observation period is assigned to be 700°C, the most probable chamber depth is about 2.5 km, as shown in Figure 4. If the data of Table 1 and Figure 4 are compared, it can be concluded that the temperature of the active crater fumaroles declined over the 1963–2005 period because of an increase in the depth of the zone of magma chamber degassing.

ACKNOWLEDGEMENTS

The authors would like to thank Dr. P.A. Hsieh (USGS) for granting the use of the HYDROTHERM version 2.2 PC software and Dr. S.E. Ingebritsen, Dr. D.O. Hayba and Dr. K.L. Kipp (USGS) for advising on the software and providing software documentation. The authors would like to thank the translator I.V. Maslovskaya (Scientific Research Geotechnological Center – RSGC, Far East Branch of Russian Academy of Science) for translating this paper in English.

REFERENCES

Ehara, S., Fujimitsu, Y., Nishijima, J., Fukuoka, K., and Ozawa, M.: Change in the thermal state in a volcanic geothermal reservoir beneath an active fumaroles field after the 1995 phreatic eruption of Kuju volcano, Japan, Proceedings, World Geothermal Congress, Turkey, (2005).

Fujimitsu, Y., Kanou, R., Nishijima, J., and Ehara, S.: Hydrothermal system after the 1990-95 eruption near the lava dome of Unzen volcano, Japan, Proceedings, World Geothermal Congress, Turkey, (2005).

Hayba, D.O., and Ingebritsen, S.E.: The computer model Hydrotherm, a three-dimensional finite-difference model to simulate ground-water flow and heat transport in the temperature range of 0 to 1,200oC, U.S. Geol. Surv. Water Res. Invest. Rep. 94-4045, (1994), 85 p.

Hurwitz, S., Kipp, K.L., Ingebritsen, S.E., and Reid, M.E.: Groundwater flow, heat transport, and water-table position within volcanic edifices: Implications for volcanic processes in the Cascade Range, J. Geophys. Res, 108, (2003), 1-1 – 1-19.

Okubo, A., Kanda, W., and Ishihara, K.: Numerical simulation of volcanomagnetic effects due to hydrothermal activity, Annuals of Disas. Prev. Res. Inst., Kyoto Univ., 49 C, (2006), 211-216.

Polyak, B.G.: Geothermal features of current volcanism region, Moskow, Nauka, (1966), 180 p. (in Russian).

Reid, M.E.: Massive collapse of volcano edifices triggered by hydrothermal pressurization, Geology, 32, (2004), 373–376.

Selyangin, O.B.: Active volcanoes of Mutnovsky geothermal region – Mutnovsky and Gorely, Magma chambers and above magma chamber zones of volcanoes. Petropavlovsk-Kamchatsky: Kamchatsky state university, (2007) (in Russian).

Trukhin, Yu. P.: Geochemistry of current geothermal processes and perspective geotechnologies, Moskow, Nauka, (2003), 375 p. (in Russian).

Utkin, I.S., Fedotov, S.A., Delemen', I.Ph., and Utkina, L.I.: The dynamics of growth and development of flowing magma chambers of Mutnovsky-Gorely group of volcanoes, their thermal fields and underground heat accumulated by them, Volcanology and seismology, 6, (2005), 11–30 (in Russian).

Vakin, Ye.A., Kirsanov, I.T., and Pronin, A.A.: Active crater of Mutnovsky volcano, Bull. Volcanol, Stations, 40, (1966), 25–35 (in Russian).

Zelensky, M.Ye., Ovsyannikov, A.A., Gavrilenko, G.M., Senyukov, S.L.: Mutnovsky volcano eruption (Kamchatka) March, 17, 2002, Volcanology and seismology, 6, (2002), 25–28.

Zelensky, M.E.: Fumarolic system of Mutnovsky, Expanded abstracts, International workshop, Mutnovsky scientific drilling project, Exploring the magma-hydrothermal connection. 24–30 September, 2006. Petropavlovsk-Kamchatsky, Russia, (2006), 46–48.